The effect of pH and collector dosage on the flotation performance of arsenopyrite and pyrite

E. Avelar[1], C. Evans[2], R. Dunne[1], K. Runge[2], and E. Manlapig[2]

[1]Curtin University, Australia
[2]University of Queensland, Australia

Flotation reagent schemes applied to both greenfield projects and brownfields gold operations are derived from extensive bench scale testwork programs targeted at maximising the recovery of gold and gold-bearing minerals at an acceptable grade for downstream processing. The reagent schemes developed are specific to the ores tested and can vary greatly. A literature review shows xanthate dosages from 5 to 600 g/t have been applied as collectors for bulk flotation of gold-bearing sulfide minerals at a pH range from 3 to 11. Research shows pH influences the formation of dixanthogen and pyrite oxidation, consequently affecting the contact angle and pyrite hydrophobicity, likewise increasing xanthate dosage promotes pyrite hydrophobicity by changing the contact angle resulting in increased pyrite recovery. This research involves performing experiments according to a Central Composite Rotatable Design using a synthetic pyrite and arsenopyrite ore system to identify flotation kinetic changes based on the xanthate dosage and pH of the slurry.

INTRODUCTION

Pyrite and arsenopyrite are the main sulfide gold-bearing minerals in most refractory gold ores, requiring a flotation concentration stage to separate it from the gangue before the refractory ore treatment that liberates and recovers the gold via cyanidation (Adams, 2005).

Flotation is a physical-chemical separation that uses particle hydrophobicity to separate valuable minerals, such as gold-bearing sulfide minerals, from gangue via bubble attachment and froth recovery (Wills & Finch, 2016). Although many sulfide gold-bearing minerals have inherent hydrophobicity, it requires the addition of reagents, for instance, activators, collectors and pH modifiers, to produce sufficient hydrophobicity for effective recovery by flotation (Adams, 2005; Fuerstenau et al., 2007; Fuerstenau et al., 1968). The flotation reagent scheme applied in greenfield gold projects and operations is usually derived from extensive bench scale programs targeting maximising gold and gold-bearing minerals' recovery at acceptable grade for downstream processes. Those reagent schemes and dosages can be very particular to the specific ore tested.

Xanthates are applied as collectors for bulk flotation of pyrite and arsenopyrite, with the objective of maximising sulfur recovery, and ultimately the gold recovery. These collectors are used in combination with strong frothers and copper sulfate or lead nitrate as the activator. In many Australian gold operations, the collector potassium amyl xanthate (PAX) is applied in dosages ranging from 20 g/t to 230 g/t. The higher collector dosages were found in operations with higher sulfur grade in the flotation feed. Copper sulfate was the most commonly applied activator with dosages ranging from 50 g/t to 150 g/t. (Kappes et al., 2013; Kappes et al., 2005; Simmons et al., 1997; O'Connor & Dunne, 1991).

The slurry pH is the most critical modifier in the flotation of pyrite and arsenopyrite because it affects pulp potential, the mechanisms of activation by copper ions and adsorption of xanthate, the dispersion of the pulp and the degree of oxidation of the sulfide minerals (Kawatra & Eisele, 2001). The optimum flotation pH for pyrite is in the range of pH 4 to 8 as it is under these conditions that dixanthogen is present on the surface of pyrite. Yet, the flotation of pyrite has shown to be possible from pH 2 to 10 (Fuerstenau et al., 2007; Fuerstenau et al., 1968). Amongst Australian operations, the flotation pH of sulfide gold ores range from 6.5 to 8 (Kappes et al., 2013; Kappes et al., 2005; Simmons et al., 1997; O'Connor & Dunne, 1991).

Fuerstenau et al. (1968) showed that the recovery of pyrite is a function of pH and increases with the rise of collector dosage in the absence of $CuSO_4$ as the activator. A similar trend was observed with the use of $CuSO_4$ at fixed pH by Monte et al. (2002) on recoveries of pyrite and arsenopyrite at similar dosages to that described by Kappes et al. (2013) and O'Connor & Dunne, (1991). However, those studies focused solely on the investigation of flotation recovery without considering the effect of reagent dosage on flotation rates and concentrate grade. A detailed analysis of the effect of reagent addition levels on the flotation rate and concentrate grade of arsenopyrite and pyrite could unlock opportunities to accelerate the flotation kinetics and improve overall flotation performance. This could be achieved by modelling the flotation response of arsenopyrite and pyrite under a suite of pH and collector conditions.

In this work, a 2-factor Central Composite Rotatable Design (CCRD) is used to determine the effect of pH and PAX dosage on the flotation response of arsenopyrite and pyrite at a fixed dosage of copper sulfate. The CCRD factorial design was selected because of its ability to provide a regression model that can be used to understand the relationship between the variables using a reduced number of experiments. CCRDs are based on 2-level factorial designs with an origin at the centre (centre point) and additional axial points apart from the centre at a distance of α (Napier-Munn, 2014). The value of α is selected to provide rotatability to the design. The value of α for rotatability is calculated by:

$$\alpha = 2^{k/4} \qquad [1]$$

Where k is the number of factors. Figure 1 shows the structure of a 3-factor CCRD (Napier-Munn, 2014).

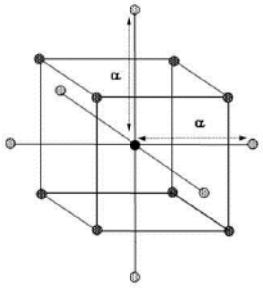

Figure 1. Structure of 3-factor CCRD (Napier-Munn, 2014).

EXPERIMENTAL

The study of arsenopyrite and pyrite flotation performance was done by performing batch flotation tests using a synthetic ore created by combining pure minerals. The advantage of using a synthetic ore system is that it allows specific effects of the mineral of interest to be identified without the interference of the complex mineralogy of a 'real' ore. The synthetic ore composition used in the flotation tests was constant at 1.6 % arsenopyrite, 3.5 % pyrite, and 95 % silica, similar to Barrick's Carlin ore's sulfide composition from North America. The minerals used in the synthetic ore mixture were prepared to create a similar size distribution and P_{80} to the Carlin ore from Barrick. The reagent regime chosen is expected to result in the recovery of both pyrite and arsenopyrite, as this is the objective when treating a Carlin style ore.

Flotation tests were performed, based on a 2-factor CCRD design, to obtain flotation performance data by measuring the mineral and water recovery as a function of time. The 14 tests performed are shown in Table 1, of which six tests were repeats (i.e. 1, 4, 7, 9, 11 and 14).

Table 1. 2-factor CCRD design test program

Run Order	Blocks	PAX dosage (g/t)	pH
1	2	165	7.0
2	2	30	7.0
3	2	165	4.0
4	2	165	7.0
5	2	300	7.0
6	2	165	10.0
7	2	165	7.0
8	1	260	4.9
9	1	165	7.0
10	1	260	9.1
11	1	165	7.0
12	1	69	4.9
13	1	69	9.1
14	1	165	7.0

Mineral samples preparation

Pyrite and arsenopyrite samples, purchased from GEO Discoveries (Geo Discoveries, 2012), were crushed individually to -850 µm and subsequently split using a rotary sample splitter. Arsenopyrite was divided into 16 g subsamples and pyrite into 35 g subsamples, which was the mass required to result in 1.6 % arsenopyrite and 3.5 % pyrite in the feed. The subsamples were sealed in individual bags and stored in the freezer at - 18°C to minimise oxidation. The purity of the purchased pyrite and arsenopyrite was tested using MLA XBSE to identify and quantify the contamination by other minerals via modal mineralogy. The MLA XBSE modal mineralogy data showed high purity levels, over 98%, of arsenopyrite and pyrite.

The silica sand was purchased from Sibelco Australia and then split into the 950g aliquots required for each flotation test using a rotary splitter. These samples are originated from Lang Lang, Victoria, Australia. It consisted of quartz Sibelco's Silica Flour 60G sand 99.7% SiO_2 with minor traces of contaminants, consisting of 0.09% Al_2O_3, 0.02% Fe_2O_3, 0.02% Ti_2O and 0.2% loss on ignition. The size distribution of the silica was determined via a Malvern sizer. The calculated P_{80} of the silica used in the testwork was 95 µm. The size distribution data showed that 52% of the silica was below 38 µm.

Mineral samples characterisation

Arsenopyrite and pyrite grinding and sizing characterisation

Before each flotation test, pyrite and arsenopyrite were ground together in a laboratory mill, achieving a solids P_{80} of 60±4 µm. The grinding error, represented by the 95% confidence interval, was determined by performing three repeat grinding tests prior to commencing the core flotation experimental work. The grinding of the sulfide minerals was performed using 75 mL of Brisbane tap water in a 20.5 cm diameter, 23.3 cm long stainless-steel rod mill for 5 minutes. The grinding media consisted of four mild steel rods having a total mass of 2841 g. The mild steel rods used were cleaned with silica in the rod mill for 5 minutes before the arsenopyrite and pyrite grinding to remove oxidised steel layers. The total mass of the mild steel rods was monitored though out the experimental program.

Product Sizing for Flotation

The arsenopyrite and pyrite individual size distribution and P_{80} was obtained by assaying arsenic and sulfur in the size fractions of the combined ground product. The assays were then converted to mineral masses and the cumulative mineral mass distribution was then calculated and interpolated to determine

the mineral specific P_{80} of arsenopyrite and pyrite, respectively. The details of the analytical assaying procedures are provided in section 2.5.

Flotation reagents preparation

The slurry pH adjustment prior to each flotation test was made using a 5% by weight solution of sodium hydroxide and a 1% by volume solution of sulfuric acid. The $CuSO_4$ used was prepared as 10 g/L solutions from solid analytical grade $CuSO_4.5H_2O$. A 100 ml of PAX solution 20 g/L was prepared daily from solid PAX, of 90% purity. The frother, Dowfroth 250, was selected due to its high dynamic foamability index (DFI) (Laskowski, 2004) and is commonly used in gold flotation operations. Frother was added undiluted to the flotation water using a micropipette prior to the addition of silica. All reagent solutions were prepared using Brisbane tap water with the composition presented in Table 2 (Queensland Urban Utilities, 2019).

Table 2. Brisbane tap water composition

Element	Aluminium	Chloride	Fe	TDS	Total Hardness	pH
ppm	0.046	62	0.011	290	120	7.7

Flotation tests

The flotation tests were performed in a 5 L bottom driven laboratory scale flotation cell with an Agitair impeller and stator. The operating parameters were: impeller speed 800 rpm, air rate 11 L/min and a froth depth of 1 cm below the cell lip. The froth was removed manually every 10 s with a scraper. The cell volume was maintained by manually adding water pre-conditioned with 30 ppm frother (135 g/t) and at the test targeted pH. All tests were run at 20 wt % solids. The dry silica was wetted in the flotation cell using 2 L of tap water pre-conditioned with the frother for approximately 2 minutes. Arsenopyrite and pyrite were added to the cell immediately after grinding with the remaining dilution water. The pH is adjusted, and the slurry was conditioned for 6 minutes to ensure the appropriate mixing of the mineral components. The pulp was conditioned with $CuSO_4$ activator 100 g/t for 2 minutes, followed by 2 minutes of conditioning with PAX before air injection. The concentrates were collected at 0.5, 1, 2, 6 and 10 minutes. These were weighed, filtered, dried at 70°C, reweighed and then subsampled for assay. The natural pulp potential (Eh) was measured after pH adjustment of the slurry, prior to activator and collector addition, and immediately after finishing the flotation test, in the flotation tailings.

Analytical procedure

The quantities of the minerals present in the concentrates and tailings of the flotation tests were determined via assay of As and S. Table 3 shows the elements assayed and the ratios used to calculate the mineral assays in the synthetic ore.

Table 3. Assayed Elements

Mineral	Formula	Assayed Element	% of Assayed Element in the Mineral
Pyrite	FeS_2	S	53.45
Arsenopyrite	FeAsS	As, S	As = 46.01, S = 19.69

The percentages of each mineral in the streams tested were calculated via element-to-mineral conversions (Webmineral 2021a,b), using the percentage weight of the assayed elements. Silica content was obtained by the difference between the sample mass and the mass of the sulfide minerals calculated via the assayed elements As and S. Arsenic was assayed via aqua regia digestion using the ICP-ES finish method, and sulfur via LECO.

RESULTS

Mineral samples characterisation

Table 4 shows the P_{80} and other physical characteristics of pyrite, arsenopyrite and silica.

Table 4. Physical characteristics of arsenopyrite and pyrite

Mineral	Arsenopyrite	Pyrite	Silica
P_{80} (µm)	61	66	95
Fraction less than 20 µm (%)	39	47	36
Density (g/cm³)	6.18	5.01	2.7
Hardness Mohs scale	5½ - 6	6 - 6½	7

Although arsenopyrite and pyrite present similar density and hardness in Table , the slight difference in hardness was sufficient to demonstrate that arsenopyrite grinds preferentially to pyrite, as it presented a finer P_{80} than the latter. This characteristic is more accentuated in real ores because of the higher density of arsenopyrite that makes it accumulate in the circulating load of grinding circuits leading to over grinding, consequently reducing the P_{80} significantly. The proportion of arsenopyrite and pyrite in the size fraction less than 20 µm presented in Table 4 was slightly higher than the silica. Therefore, it is expected that entrainment may contribute to the overall recovery of the sulfide minerals.

Flotation repeatability

The flotation reproducibility in the 2-factor CCRD was assessed via 6 repeats of the centre point at pH 7 and PAX dosage of 165 g/t. The repeats were performed as part of the main body 2-factor CCRD in blocked order, which enables one to determine whether there is any systematic error in the experimental program with time. The reproducibility of the flotation tests performed is shown in Table 5 by the relative confidence interval at 95% confidence (indicated as CI%) as a proportion of the mean. The error obtained in the first 0.5 minutes of flotation was the major contributor to the variability of the tests. No systematic error with time was detected.

Table 5. Flotation recovery and grade repeatability

Flotation Time (minutes)	Cumulative Recovery %								Cumulative Grade %			
	Solids		Water		Pyrite		Arseno-pyrite		Pyrite		Arseno-pyrite	
	Ave	CI %	Ave	CI %	Ave	CI %	Ave	CI %	Ave	CI %	Ave	CI %
0.5	2.3	18.3	1.0	29.4	38.8	20.1	39.8	17.8	58.8	4.1	25.6	12.3
1.0	4.1	10.3	2.3	17.6	67.8	7.5	67.4	8.1	56.9	5.4	23.8	8.9
2.0	5.2	7.9	4.0	15.1	82.5	3.6	80.8	3.7	55.1	6.7	22.7	9.0
6.0	6.9	6.5	8.1	9.4	98.2	0.9	96.7	0.4	49.1	6.8	20.3	7.6
10.0	7.7	6.1	13.0	7.9	99.5	0.3	98.1	0.5	45.0	6.2	18.7	6.5

The variability of pyrite was found to be higher than the arsenopyrite due to the higher variability of the sulfur assays compared to arsenic. Pyrite will also be more prone to error because it is more susceptible to propagation of error during the metal-to-mineral conversion process. Arsenopyrite is only dependent on the arsenic assay. The pyrite assay, on the other hand, is calculated using a sulfur assay which has been corrected to remove the sulfur in arsenopyrite which in turn is dependent on the accuracy of the arsenic assay.

Pyrite and Arsenopyrite

Recovery versus time analysis

Firstly, the effect of pH and collector dosage in the arsenopyrite and pyrite recovery is evaluated through the recovery versus time (kinetic) curves in Figure 2 and Figure 3. Arsenopyrite and pyrite

presented analogous kinetic behaviour as the curves shown in Figure 2 and Figure 3 follow a similar trend.

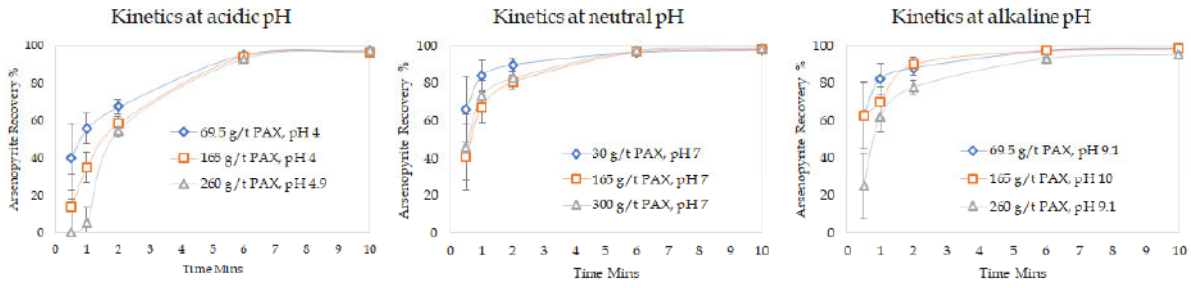

Figure 2. Cumulative recovery of arsenopyrite in the 2-factor CCRD varying collector dosage at acidic, neutral and alkaline pH

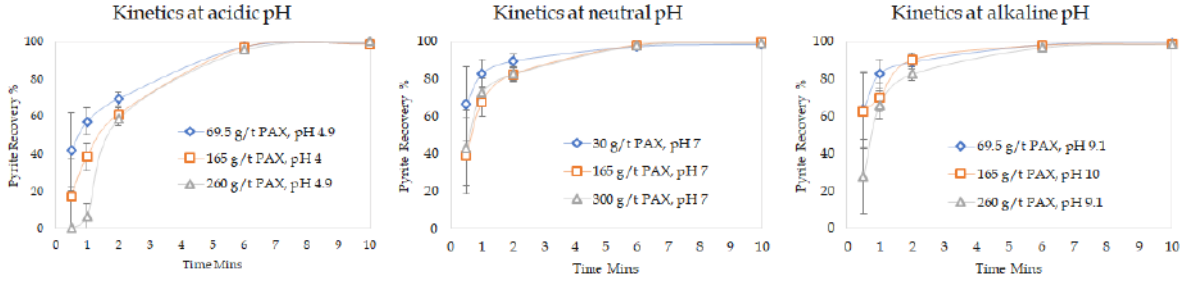

Figure 3. Cumulative recovery of pyrite in the 2-factor CCRD varying collector dosage at acidic, neutral and alkaline pH

There are two characteristics that can be evaluated using the kinetic curves – the final recovery that is achieved by the end of the test and the speed of flotation (or flotation kinetics), which is a measure of how fast the system reaches its final recovery value. In terms of the overall recovery value, all tests achieve near to 100% recovery of pyrite and arsenopyrite after 10 minutes of flotation. However, there are noticeable changes in the flotation kinetics.

The slowest flotation kinetics for arsenopyrite and pyrite were observed at acidic pH (the time taken to get to the final recovery is longer). For a particular pH condition, the fastest kinetics are observed when the collector dosage is low. Under acidic and alkaline conditions, an increase in collector dosage decreases the flotation kinetics. While at natural pH, no significant difference in the flotation kinetics is observed by increasing the collector dosage beyond 165 g/t.

Flotation kinetics analysis

To enable a quantitative assessment of flotation kinetic performance, the flotation rate constants of arsenopyrite and pyrite for the 14 tests of the 2-factor CCRD were estimated based on equation 2.

$$R = R_{\infty}\,(1-e^{(-kt)}) \qquad [2]$$

Where R is the flotation recovery at a given time, R_{∞} is the final flotation recovery, t is the flotation time, and k is the flotation rate constant. It was not considered necessary to include an entrainment mechanism in the recovery equation. This was because entrainment recovery as predicted using equation 3 referenced from Savassi (1998) predicted that pyrite and arsenopyrite recovery by entrainment in the tests was less than 0.7% and 2.6%, respectively.

$$R_{ent} = \frac{1-R_{overall}}{1-R_{water}} . ENT_m . R_{water} \quad [3]$$

where ENT_m is the degree of entrainment of mineral m, R_{ent} is the recovery of mineral m by entrainment, $R_{overall}$ is the recovery of mineral m by both entrainment and true flotation, and R_{water} is the water recovery. The degree of entrainment parameter used in these calculations was estimated based on the silica entrainment.

The calculated flotation rates obtained from Equation 2 were grouped according to pH and collector dosage levels categorised as low (< 60 g/t), intermediate (165 g/t) and high (> 250 g/t), and are shown in Table 6. The final flotation recoveries used in Equation 2 to calculate the flotation rates in Table 6 are presented in Table 7.

Table 6. Calculated flotation rates of arsenopyrite and pyrite

pH/ PAX dosage	k arsenopyrite (k_{aspy}) min^{-1}			k pyrite (k_{py}) min^{-1}		
	Low	Intermediate	High	Low	Intermediate	High
Acidic	0.65	0.52	0.41	0.67	0.54	0.43
Neutral	1.91	0.89	1.09	1.78	0.91	1.05
Alkaline	1.65	1.37	0.87	1.63	1.36	0.93

Table 7. Final flotation recovery of arsenopyrite and pyrite

pH/ PAX dosage	R_∞ arsenopyrite %			R_∞ pyrite %		
	Low	Intermediate	High	Low	Intermediate	High
Acidic	98.6	98.0	98.9	98.7	100.0	99.8
Neutral	98.3	99.0	99.1	98.2	99.2	99.2
Alkaline	98.6	98.8	98.2	99.4	98.1	98.2

Flotation rate constants of pyrite and arsenopyrite were very similar for a particular set of pH and collector dosage conditions. At low collector dosage, pyrite and arsenopyrite presented low flotation kinetics at acidic conditions, having the highest kinetic rate shown at neutral pH and slightly lower kinetics at alkaline pH. Similar behaviour is observed at high collector dosages, however, at lower flotation rates. At intermediate collector dosage, the flotation rate increased with pH.

Predictive flotation kinetic modelling

The effect of collector dosage and pH in the calculated flotation rate of arsenopyrite and pyrite for each of the 14 tests was investigated by regression models obtained using the stepwise regression tool of Minitab® 19 software. Table 8 shows the model statistics of the regression model of the flotation rate constants of pyrite and arsenopyrite. The models shown in Table 8 presented a high coefficient of determination (R^2) and low predictive uncertainty.

Table 8. Model statistics of the flotation rate constant

Model Summary	Standard error	Confidence Interval at 95%	Predictive uncertainty	R^2
Pyrite	0.18	0.19	0.98	83%
Arsenopyrite	0.21	0.22	1.37	80%

Figure 4 shows a reasonable fit between the model predictions and the measured flotation rate values. Hence, demonstrating that the models are capable of predicting the flotation rates of pyrite and arsenopyrite well.

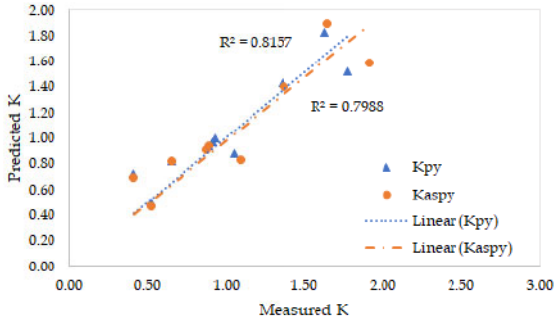

Figure 4. Arsenopyrite and pyrite flotation model predictions versus observations

The regression equations of arsenopyrite and pyrite flotation rates are presented as equations 4 and 5. The statistics of the coefficients for the flotation rate constant regressions for arsenopyrite and pyrite are shown respectively in Table 9 and Table 10, respectively.

$$K_{aspy} = -0.568 + 0.3391\ pH + 0.000015\ PAX^2 - 0.001108\ pHxPAX \quad [4]$$

$$K_{py} = -0.474 + 0.3116\ pH + 0.000013\ PAX^2 - 0.000950\ pHxPAX \quad [5]$$

Where pH is the absolute pH of the test and PAX is the dosage of potassium amyl xanthate in grams per tonne of feed. The flotation rate regressions of arsenopyrite and pyrite present in equations 2 and 3 have similar terms and the magnitude of the coefficients are similar.

Table 9. Model coefficients and statistics of the flotation rate constant of arsenopyrite

Term	Coefficients	SE of Coefficient	Coded Coefficients	P-value
Constant	-0.568	0.0554	1.0214	0.000
pH	0.03391	0.105	0.564	0.000
PAX^2	0.000015	0.171	0.392	0.045
pH x PAX	-0.001108	0.192	-0.667	0.006

Table 10. Model coefficients statistics of the flotation rate constant of pyrite

Term	Coefficients	SE of Coefficient	Coded Coefficients	P-value
Constant	-0.474	0.0476	1.0179	0.000
pH	0.3116	0.0900	0.5185	0.000
PAX^2	0.000013	0.147	0.323	0.052
pHxPAX	-0.000950	0.165	-0.572	0.006

According to the data shown in Table 9 and Table 10, the flotation rate of arsenopyrite and pyrite are affected significantly by the PAX dosage and pH, as the P-values of the terms pH, PAX dosage squared, and the interaction of pH x PAX dosage are lower than 0.05. The most significant predictors for the flotation rate constant of arsenopyrite and pyrite are the constant, followed by the interaction of pH x PAX dosage, the pH and the square of PAX dosage, as shown by the standardised coefficients. The interactive effect of pH and PAX and the square of PAX dosage terms introduce curvature to the response surface of the flotation rate constant of arsenopyrite and pyrite, as shown in Figure 5.

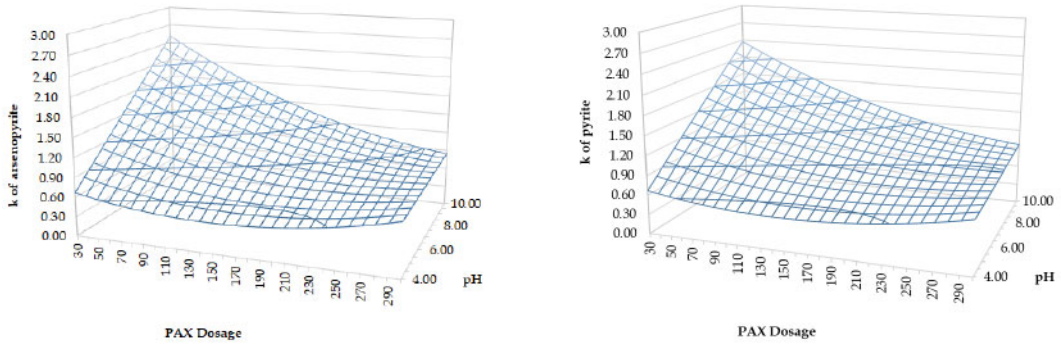

Figure 5. Response surface of the flotation rate constant of arsenopyrite and pyrite

The gradient of variation of the flotation rate constant of arsenopyrite and pyrite versus the pH throughout the range of collector dosage tested shows that low PAX dosages and neutral to alkaline pH would increase the flotation rate. The relationship is accentuated because of the significance of the terms pHxPAX and PAX^2, as shown in Figure 5. The highest flotation rates for arsenopyrite and pyrite in Figure 5 were achieved at pH 10 and 30 g/t.

Overall flotation performance

Grade-recovery curves were created to assess the overall flotation performance of the system. The curves in Figure 6 and Figure 7 were grouped by pH (acidic, neutral and alkaline) and PAX dosage (low, intermediate and high) to identify the best reagents condition that maximises the selectivity of the system.

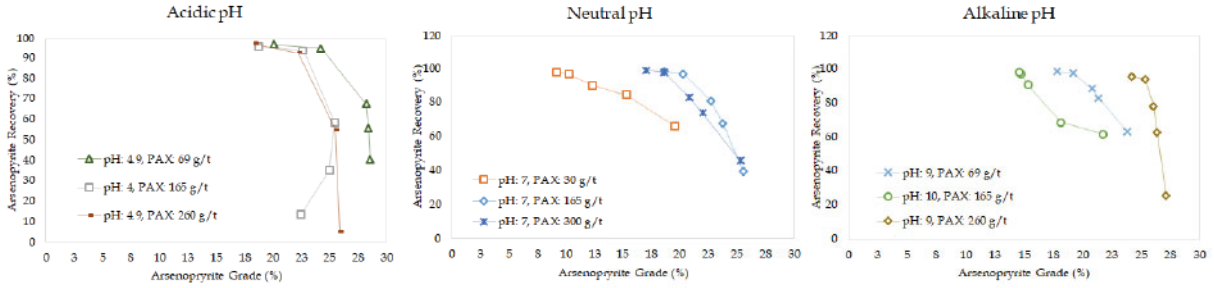

Figure 6. Arsenopyrite grade-recovery curves

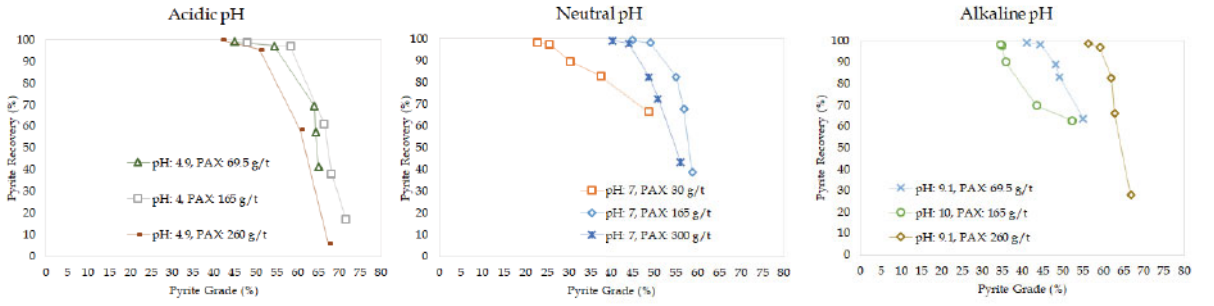

Figure 7. Pyrite grade-recovery curves

With pyrite and arsenopyrite exhibiting similar flotation kinetics in the system, grade at a particular sulfide recovery will be a function of how much silica is being recovered under that condition. High grades, at a particular recovery, will be achieved when silica recoveries are low and vice versa. According to Figure 6 and Figure 7, a high collector dosage promoted the selectivity of pyrite and

arsenopyrite against silica at alkaline pH. Intermediate PAX dosages showed better selectivity of arsenopyrite and pyrite against silica at neutral pH. In acidic pH, low collector dosage improved the selectivity of arsenopyrite. This behaviour differs from pyrite, which showed no further improvement of selectivity by reducing the PAX dosage below 165 g/t of PAX at acidic pH. The poorest selectivity of arsenopyrite and pyrite with silica was found at pH 7 when 30 g/t of PAX was used.

Pyrite and Arsenopyrite Selectivity

Pyrite and arsenopyrite exhibit similar flotation kinetics (Table 6) and this means they are being recovered at the same recovery rate in the flotation experiments. This is evident in the arsenpyrite versus pyrite selectivity curves which are shown in Figure 8. The arsenopyrite/pyrite selectivity curves overlap and essentially fall on the 45 degree diagonal. Therefore selective separation of arsenopyrite and pyrite is not possible under the flotation conditions tested.

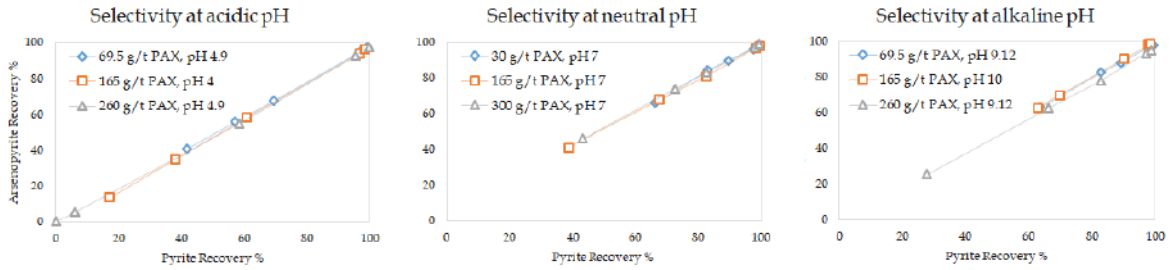

Figure 8. Arsenopyrite and pyrite selectivity at acidic, neutral and alkaline conditions, with PAX dosage ranging from 30 g/t to 300 g/t

Results of Eh Measurements

The natural pulp potential (Eh) was monitored during the conditioning stage of the flotation tests and after test completion. The measurements of pulp potential versus the final flotation recoveries and flotation rates of arsenopyrite and pyrite in the range of pH and PAX concentration tested are shown in Figure 9.

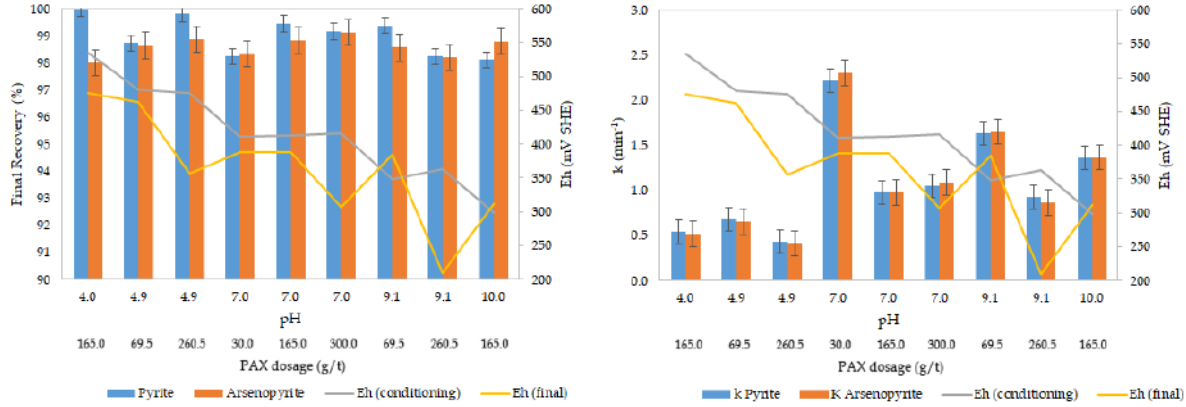

Figure 9. Pulp potential, flotation recovery and rates as a function of pH and PAX dosage

In Figure 9, the pulp potential during the conditioning stage ranged from +299 to +535 mV (SHE) and declined with the increase in pH (grey trend). Collector dosage is not expected to affect the masurements performed during the conditioning stage, as the measurement was taken before collector addition. In contrast, the pulp potential trend observed at the completion of the test shows a decrease in Eh with an increase in collector dosage. No significant difference in arsenopyrite and pyrite recovery with pulp potential was observed in Figure 9. However, the lowest flotation rates of arsenopyrite and pyrite were observed at low pH.

Silica and Water Recovery

With their being no selectivity difference between pyrite and arsenopyrite, the grade scenarios shown in Figure 6 and Figure 7 will be associated with how much silica is being recovered at each test condition. As silica is fully liberated and is expected not to float, its recovery is expected to be largely via entrainment, which will be proportional to water recovery. The water recovery estimated for each flotation concentrate was calculated by dividing the mass of water recovered into the concentrate by the total amount of water in the tailing and that measured in all concentrates. This is equivalent to the amount of water recovered per mass of water in the feed and that added during the test to keep the cell level constant.

Figure 10 shows the cumulative silica recovery versus the cumulative water recovery to each concentrate in all tests performed. If entrainment was the primary mechanism of recovery of silica, it would be expected that its recovery would be proportional to that of water recovery, with a slope equal to its degree of entrainment, a parameter which accounts for the classification of solids with respect to water across the froth phase (see equation 3) (Zheng et al., 2006; Johnshon, 2005; Lynch et al., 1981; Engelbrecht & Woodburn, 1975). This is observed for all tests except for the run performed at 30 g/t of PAX and pH 7, Run 2, which showed an increased silica recovery compared to water recovery.

The average slope of the relationship between silica and water recovery (i.e. overall degree of entrainment) for all tests, but Run 2, is 0.27, whereas the slope for Run 2 is about 0.90. The expected overall degree of entrainment in a batch test system can be estimated using the size distribution of the silica and typical degree of entrainment values for each size of a non sulphide gangue published by Johnson, 2005. This value calculated for the silica used in these experiments is 0.24 which is very similar to the measured 0.27 value. It can therefore be concluded that silica in the majority of tests is being recovered only by entrainment whereas the silica in the 30 g/t of PAX and pH 7 test is being recovered due to a mechanism other than entrainment because it exhibits an overall degree of entrainment that is far above what is expected. It should be noted that the relationship between silica and water recovery presented by Run 2 is not linear.

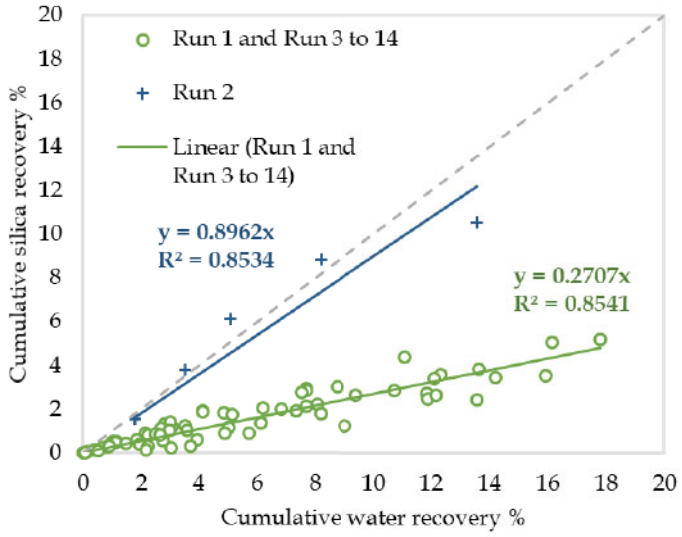

Figure 10. Cumulative water recovery versus cumulative solids and silica recovery

With water recovery being the driver for silica recovery in all but Run 2, the data were investigated to determine the degree to which water recovery changed as pH and collector dosage was varied in the experiments. Figure 11 shows the cumulative water recovery as a function of collector dosage at acidic, neutral and alkaline pH. No significant change in water recovery was observed by varying the collector

dosage at acidic and neutral pH. However, significant changes are observed at alkaline pH, with water recovery being optimal under intermediate collector dosage conditions.

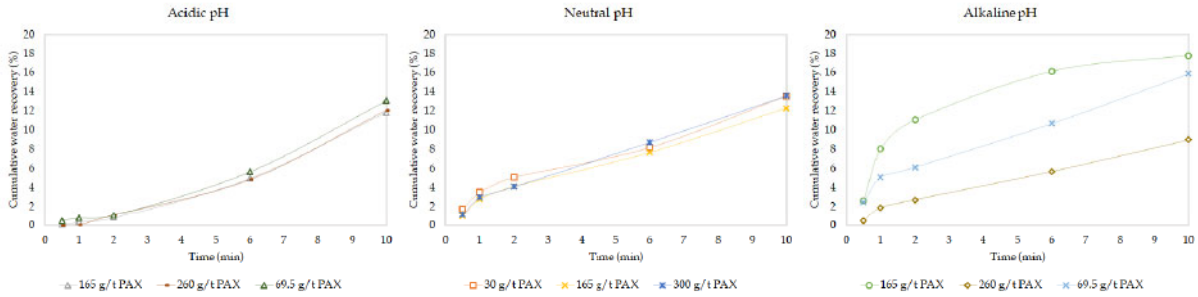

Figure 11. Cumulative water recovery by time at low, intermediate and high PAX dosage at acidic, neutral and alkaline pH

Because of the orthogonality of the experimental design, it is possible to average the water recovery results at each pH condition, to compare and provide insight into the underlying effects of pH. The averaged cumulative water recovery versus time at acidic, neutral and alkaline pH conditions are displayed in Figure 12. According to Figure 12, the amount of water reporting to concentrate is rising in a linear systematic manner as the pH is increased in the system.

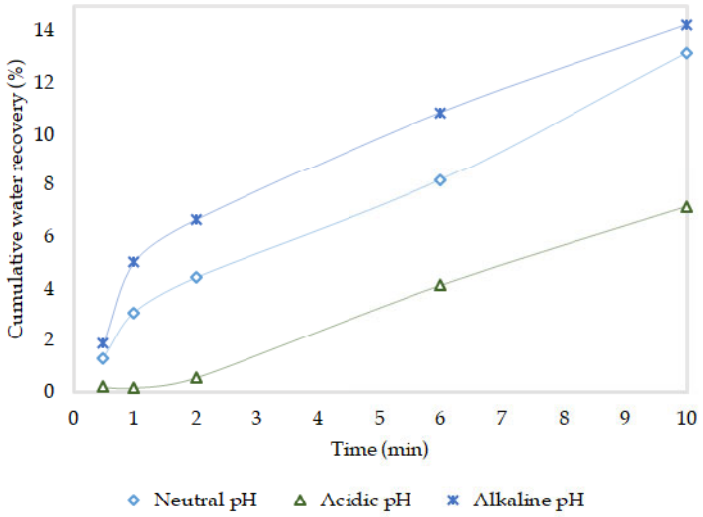

Figure 12. Averaged cumulative water recovery by time at acidic, neutral and alkaline pH

DISCUSSION

Across the range of pH and PAX dosages tested, almost complete recovery of arsenopyrite and pyrite was observed in the batch flotation tests after 10 minutes of flotation, as shown in Figure 2 and Figure 3. Differences, however, were observed in flotation behaviour, most notably, there were significant effects on flotation kinetics and the concentrate grade achieved.

The slowest flotation kinetics of arsenopyrite and pyrite were observed at acidic pH. This result was unexpected because, at these conditions, the Cu^{2+} from $CuSO_4$ is reduced to Cu^{+}, and should enhance arsenopyrite and pyrite's hydrophobicity (Moslemi & Gharabaghi, 2017; López Valdivieso et al., 2006; Sirkeci, 2000; Gaudin, 1957). According to Fuerstenau et al. (2007), the optimum flotation pH for pyrite is expected to be in the range of pH 4 to 8 due to dixanthogen's presence on its surface. At alkaline pH values, dixanthagen is expected to be thermodynamically unstable due to the high concentrations of

OH^- (Fuerstenau et al., 2007). High collector dosages were also expected to increase particle hydrophobicity, accelerating the flotation rate of the sulfide minerals. This largely didn't occur with elevated kinetics achieved at lower levels of collector dosage.

The pulp potential in the experiments conducted ranged from +299 to +535 mV (SHE) and appeared not to influence the flotation recoveries of arsenopyrite and pyrite (refer to Figure 9). These results agree with Valdivieso et al. (2006) that found high recoveries of arsenopyrite above a pulp potential of +200 mV (SHE). In addition, previous studies have found that the recovery of pyrite is possible at an Eh range from 0 to 300 mV (SHE) in the studied pH range (Hu et al., 2010; Ralston, 1991; Gebhardt and Richardson, 1987; Chander, 1985). The slowest flotation rate of arsenopyrite and pyrite were observed at acidic pH, where the highest pulp potentials were achieved. At acidic pH, the Eh values found were roughly above 450 mV (SHE). These Eh values exceeded the potential that favours the adsorption of xanthate on copper activated pyrite, according to He et al. (2005).

One of the potential reasons for the unexpected kinetic results is that highly hydrophobic particle surfaces may be resulting in poor froth stability (Wiese et al., 2011). Bursting bubbles may be returning particles from the froth back to the pulp phase, reducing the rate of collection to concentrate. Recovery of water to concentrate has been used as an indicator of froth stability (Neethling and Brito-Parada, 2018; Hardler and Cilliers, 2009), with unstable bursting froths exhibiting lower water recoveries. Trends in the cumulative water recovery results do indicate a more stable froth created with an increase in system pH. The faster kinetics as pH increases may therefore be a consequence of improved froth stability. Collector dosage does not, however, result in a discernible change in water recovery at low and neutral pH. At high pH, significant changes in water recovery are observed with changing collector dosage, but the relationship is not linear, with the most stable froth being created at intermediate collector dosage. It is therefore concluded that the poor kinetics observed at high collector dosage (especially at acidic and neutral pH) is likely to be related to a change in hydrophobicity of the particle surfaces, the reason for which requires more study.

The concentrate grade versus recovery relationships (Figure 6 and Figure 7) were found to vary significantly with a change in pH and collector dosage. This is a consequence of these conditions changing not only the rate of flotation of the iron sulfides but also the recovery rate of silica. Silica recovery was largely found to be via entrainment, with a linear relationship observed between water and silica recovery in all but one test (Figure 10). Water recovery was found to increase with pH and be independent of collector dosage under acidic and neutral pH conditions. Under alkaline conditions, water recovery was highest at intermediate collector dosage conditions and lowest at high collector dosage. Changes in water recovery are postulated to be due to the pH and collector dosage affecting the froth stability. These changes in water recovery consequently affect silica recovery rates and thus contribute to the variation in concentrate grade produced in the test series.

There was evidence, however, of a mechanism other than entrainment affecting silica recovery for the test performed at 30 g/t of PAX and pH 7. Silica recovery in this test did not follow the classical linear relationship with water recovery observed at all the other test conditions and was much higher than expected. This suggests that these conditions have rendered the silica surface hydrophobic, resulting in much higher flotation recoveries.

Fornasiero & Ralston (2005) have reported that the silica surface can be rendered hydrophobic through the activation via copper ions. In their experiments, they observed under neutral to acidic conditions and at compatible concentrations of $CuSO_4$ and xanthate an increase in recovery of Cu^{2+} activated silica by flotation. Xanthate and Cu(I)-xanthate molecules were found on the surface of the silica. This effect was not observed when the dosage of xanthate exceeded the dosage of copper. In this study, the test presenting abnormal silica recovery was under similar conditions to that presented by Fornasiero & Ralston (2005). In Run 2 performed at 30g/t of PAX and pH 7, the $CuSO_4$ dosage of 100 g/t (used in all tests) exceeds that of the xanthate addition and pH is neutral. Therefore, the abnormal silica recovery observed could be due to the activation of silica and recovery due to true flotation.

CONCLUSIONS

Almost complete recoveries of arsenopyrite and pyrite were achieved across the spectrum of pH and collector dosages tested in the experiments presented in this paper. It was possible, however, to change the grade versus recovery response by using pH and collector dosage to manipulate the kinetics of arsenopyrite and pyrite, as well as the recovery of silica. The kinetics of arsenopyrite and pyrite could be maximised by using conditions that maximise water recovery and by using low collector dosage. The faster kinetics at high water recovery may be a consequence of improved froth stability. However, further investigation is required to conclusively prove this link. Silica recovery can be minimised by using conditions that minimise water recovery and thus recovery by entrainment. The optimal grade versus recovery was achieved at high PAX dosage and alkaline pH as it resulted in reasonable flotation rates of the iron sulfides but low water and thus silica recoveries.

Silica was also found to be rendered floatable when the copper to xanthate dosage ratio was high, and thus this condition should be avoided. Further investigation is required to optimise the copper and xanthate ratio for systems that require low xanthate collector addition.

This paper has demonstrated the different mechanisms that can be in play when performing experiments using a pyrite/arsenopyrite ore and how they can be manipulated to achieve optimum performance by varying pH and reagent dosage rates.

ACKNOWLEDGMENTS

The authors acknowledge the support from Barrick Gold Corporation through the Amira P9P project and the Australian Government Research Training Program Scholarship.

REFERENCES

Adams, M. D. (2005). *Advances in Gold Ore Processing*. Amsterdam: Elsevier.

Chander, S. (1985). Oxidation/reduction effects in depression of sulfide minerals— a review. *Miner. Metall. Process.* 2(1):26.

Gebhardt, J.E., and P.E. Richardson. 1987. Differential flotation of a chalcocite-pyrite particle bed by electrochemical control. *Miner. Metall. Process.* 4:140.

Geo Discoveries, G. (2012). *Geo Discoveries*. Retrieved from Geo Discoveries: http://www.geodiscoveries.com.au/

Engelbrecht, J. A., & Woodburn, E. T. (1975). The effect of froth height, aeration rate and gas precipitation on flotation. *J. South Afr. Inst. Min. Metall., 76*(special issue), 125-132.

Fornasiero, D., Ralston, J. (2005). Cu(II) and Ni(II) activation in the flotation of quartz, lizardite and chlorite. *International Journal of Mineral Processing*, 76, 75-81.

Fuerstenau, M.C., Jameson, G.J., & Yoon, R.H. (2007). *Froth Flotation: A Century of Innovation*. Society for Mining, Metallurgy, and Exploration, Littleton, Colo.

Fuerstenau, M. C., Kuhn, M. C., & Elgillani, D. A. (1968). The Role of Dixanthogen in Xanthate Flotation of Pyrite. T*ransactions of the American Institute of Mining, Metallurgical and Petroleum Engineers*(241), 148-156.

Gaudin, A.M. (1957). *Flotation*. New York, USA: McGraw-Hill Book Co.

Hadler, K., Cilliers, J.J., 2009. The relationship between the peak in air recovery and flotation bank performance. *Minerals Engineering*. 22, 451–455.

He, S., Fornasiero, D., Skinner, W., 2005. Correlation between copper-activated pyrite flotation and surface species: Effect of pulp oxidation potential. *Minerals Engineering*. 18, 1208-1213.

Hu, Y., Sun, W., Wang, D. (2010). *Electrochemistry of flotation of sulphide minerals*, Springer Science & Business Media.

Johnson, N. W. (2005). A review of entrainment mechanism and its modelling in industrial flotation process, *CIM Bulletin, 80* (899): 113-117.

Kappes, R., Simmons, G. L., & LeVier, K. M. (2005). Pyrite activation in Amyl Xanthate flotation with nitrogen. *Centenary of Flotation Symposium* (999-1004). Brisbane: The Australasian Institute of Mining and Metallurgy.

Kappes, R., Fortin,C., & Dunne, R. (2013). Current status of the chemistry of gold flotation in industry. *CIM Journal*, 4 (3), 1-7.

Kawatra, S., & Eisele, T. C. (2001, January). *Fundamental principles of froth flotation.* Retrieved from https://www.researchgate.net/publication/281944301_Fundamental_principles_of_froth_flotation

Laskowski, J. S. (2004). Testing Flotation Frothers. *Physicochemical Problems of Mineral Processing*, 18, 13-22.

López Valdivieso, A., Sánchez López,, A. A., Ojeda Escamilla, C., & Fuerstenau, M. C. (2006). Flotation and depression control of arsenopyrite through pH and pulp redox potential using xanthate as the collector. *International Journal of Mineral Processing*, 27-34.

Lynch, A. J., Johnson, N. W., Manlapig, E. V., Thorne, C. G. (1981). *Mineral and coal flotation circuits - Their simulation and control*. Elsevier: Amsterdam.

Monte, M. B., Dutra, A. J., Albuquerque, C. R., Tondo, L. A., & Lins, F. F. (2002). The influence of the oxidation state of pyrite and arsenopyrite on the flotation of an auriferous sulfide ore. *Minerals Engineering*, 15(12), 1113-1120.

Moslemi, H., Gharabaghi, M. (2017). A review on electrochemical behavior of pyrite in the froth flotation process. *Journal of Industrial and Engineering Chemistry*, 47, 1-18.

Napier-Munn, T. J. (2014). *Statistical Methods for Minerals Engineers.* Indooroopilly, QLD, Australia: Julius Kruttschnitt Mineral Research Centre .

Neethling, S.J., Brito-Parada, P.R. (2018). Predicting flotation behaviour – The interaction between froth stability and performance. *Minerals Engineering, 120*, 60-65.

O'Connor, C. T., & Dunne, R. C. (1991). The Practice of Pyrite in South Africa and Australia. *Minerals Engineering, 4*, 1057-1069.

Ralston, J. (1991). Eh and its consequences in sulphide mineral flotation. *Minerals Engineering, 4* (7–11), pp. 859-878.

Savassi, O.N., *Direct Estimation of the Degree of Entrainment and the Froth Recovery if Attached Particles in Industrial Cells.* 1998, University of Queensland: Brisbane, Australia.

Simmons. , G. L. (1997). Flotation of Auriferous Pyrite Using Santa Fe Pacific Gold's N2TEC Flotation Process. *Society for Mining, Metallurgy & Exploration*, 9.

Sirkeci, A.A. (2000). The flotation separation of pyrite from arsenopyrite using hexyl thioethylamine as collector. *International Journal of Mineral Processing*, 60 (3), 263-276.

UrbanUtilities (2019). 2018/19 Drinking Water Quality Management Plan Report. Retrieved from: Water quality data - Queensland Urban Utilities

Webmineral. (2021, April 18)a. Retrieved from: Arsenopyrite Mineral Data (webmineral.com)

Webmineral. (2021, April 18)b. Retrieved from: Pyrite Mineral Data (webmineral.com).

Wiese, J., Harris, P., Bradshaw, D. (2011). The effect of the reagent suite on froth stability in laboratory scale batch flotation tests. *Minerals Engineering*, *24*(9), 995-1003.

Wills, B. A., & Finch, J. (2016). *Wills' Mineral Processing Technology.* Amsterdam: Elsevier.

Zheng, X., Johnson, N. W., & Franzidis, J. P. (2006). Modelling of entrainment in industrial flotation cells: Water recovery and degree of entrainment. *Minerals Engineering*, 1191-1203.

Erica Cristina Avelar

Research Engineer
Curtin University

Erica Avelar is a Research Engineer at the Gold Technology Group conducting research on the Mineral Processing Theme, under the ARC Centre of Excellence for Enabling Eco-Efficient Beneficiation of Minerals, Curtin University Node, Perth, Australia. She has over ten years of experience working for engineering companies across Australia and Brazil in Gold, Copper, Nickel Laterite, Phosphate and Iron Ore projects, and as a flotation plant metallurgist in a gold operation in Australia. She recently finished her PhD in 2019 at the University of Queensland in Mineral Beneficiation, focusing on gold pyritic ore flotation under the Amira P9P project.